

VDLM: Variable Diffusion LMs via Robust Latent-to-Text Rendering

Shuhui Qu

Stanford University

shuhuiq@stanford.edu

Abstract

Autoregressive language models decode left-to-right with irreversible commitments, limiting revision during multi-step reasoning. We propose **VDLM**, a modular variable diffusion language model that separates semantic planning from text rendering. VDLM applies LLaDA-style masked diffusion over semantic variable embeddings to enable iterative refinement in latent space, then post-trains the planner with trajectory-aware optimization using embedding-space rewards and values, avoiding text decoding inside the RL loop. To convert planned embeddings back to text, we use a **Vec2Text** renderer and introduce **embedding perturbations** to robustify decoding under planner noise. Across nine benchmarks spanning general reasoning, math, and code, VDLM is competitive in pre-training and yields substantial post-training improvements on long-form generation tasks, outperforming other baselines. These results highlight the effectiveness of embedding-space post-training and robust latent-to-text rendering for diffusion language modeling.

1 Introduction

Multi-step reasoning and long-form generation remain challenging regimes for modern language models, especially when solutions require revising intermediate decisions rather than extending a locally consistent prefix(Schmidt, 2019; He et al., 2021; Huang et al., 2023). Autoregressive (AR) based language models currently dominate the modeling paradigm for large language models (LLMs)(Minaee et al., 2024; Prabhudesai et al., 2025). AR based LLM decode left-to-right with irreversible commitments (Brown et al., 2020; Touvron et al., 2023; Achiam et al., 2023). This *sequential commitment* makes revision expensive: correcting an early mistake typically requires restarting, branching, or relying on external search procedures. In long-horizon reasoning (e.g., mathematics or

code), small local errors can cascade, because later tokens must condition on previously committed prefix tokens(Arora et al., 2022; He et al., 2021; Yao et al., 2023).

Recent work has tried to mitigate these issues by encouraging explicit intermediate reasoning (e.g., Chain-of-Thought, Tree-of-Thought) and sampling-based exploration (Wei et al., 2022; Wang et al., 2022; Yao et al., 2023). While these methods improve success rates in many settings, they do not fundamentally change the decoding pattern: the model commits token-by-token, and exploration remains limited by the inability to *revise* already produced text without re-generating(Yu et al., 2025; Xiong et al., 2025).

Diffusion-style generation offers a complementary perspective: instead of committing left-to-right, a model iteratively refines a partially observed representation (Ho et al., 2020; Austin et al., 2021). Diffusion language models such as LLADA scale this idea by learning to recover randomly masked tokens and sampling via repeated (re-)masking and denoising (Nie et al., 2025; Bie et al., 2025; Wang et al., 2025b). However, token-level refinement is still costly when outputs are long: the refinement unit is the token, so the model repeatedly solves a high-dimensional discrete reconstruction problem. Moreover, semi-autoregressive / block diffusion variants reduce wall-clock latency but can degrade quality for long segments, since errors introduced within a block are harder to correct once the block is committed (Nie et al., 2025; Israel et al.; Wang et al., 2018; Lu et al., 2025).

We address this tension by shifting diffusion *above tokens*. Our key premise is that long-form generation should be driven by a *short, structured planner* and a *strong renderer* that faithfully reconstructs text from the plan. Concretely, we propose **VDLM**, a *variable diffusion language model* that separates **semantic planning** from **text rendering**. VDLM operates on a sequence of continuous se-

mantic variable embeddings, which are constructed as question blocks, answer options, or reasoning concept segments, and refines these embeddings with masked denoising. This yields a much shorter refinement horizon than token diffusion while retaining the ability to revise and globally coordinate decisions.

Our framework consists of three components:

1. **Variable diffusion planning.** We apply LLADA-style masked diffusion to a matrix of variable embeddings, iteratively refining a latent plan V in continuous space (Nie et al., 2025).
2. **Embedding-space post-training.** To align the planner with downstream task metrics, we adapt TRACERL to latent variable space (Wang et al., 2025b). Both the reward signal and the value function are computed from variable embeddings. There is *no text decoding inside the RL loop*, making post-training efficient even when rendering is expensive.
3. **Robust rendering via noise injection VEC2TEXT.** We invert planned embeddings back to text using VEC2TEXT (Morris et al., 2023a). Since planner outputs are noisier than clean encoder embeddings, we perturb embeddings during renderer training (via L_2 noise) and train the corrector to recover the exact target text, substantially improving robustness under planner-induced distribution shift.

A central motivation of this paper is that **rendering quality is the bottleneck** for long outputs: improving the latent-to-text renderer yields substantially larger gains than semi-AR token-level rendering when segments become long. VDLM explicitly targets this bottleneck by pairing semantic-unit planning with a robustly trained renderer trained to withstand latent noise.

Results overview. Across nine benchmarks spanning general knowledge, reasoning, mathematics/science, and code, VDLM is competitive in the pre-training setting and improves markedly after post-training. Notably, SFT+RL post-training in embedding space yields strong long-form gains. These results support the thesis that semantic-unit diffusion planning can be effectively aligned without decoding in the RL loop, and that robust latent-to-text rendering is decisive for long-sequence performance.

The rest of the paper is organized as following: Section 3 introduces VDLM, including variable construction, the LLADA-style masked denoiser, TraceRL-style embedding-space post-training, and robust VEC2TEXT rendering. Section 4 presents experimental results on nine benchmarks together with ablations and efficiency analysis. Section 5 discusses implications, limitations, and future directions.

2 Related Work

2.1 Masked diffusion language models

Diffusion-style sequence models replace left-to-right decoding with iterative denoising under a forward corruption process, enabling global refinement rather than prefix-locked commitments. Early discrete or masked formulations include D3PM-style discrete diffusion and masked-token denoising frameworks (Austin et al., 2021; Peebles and Xie, 2023). For text generation, Diffusion-LM explores diffusion formulations for language modeling and controllable generation in token space (Li et al., 2022; Cheng et al., 2025; He et al., 2023). More recently, masked diffusion LMs have improved scalability and sampling practicality. MDLM develops simple masked diffusion objectives for language with strong empirical performance (Sahoo et al., 2024; Ye et al., 2025). LLADA scales masked diffusion for language and supports multiple decoding strategies (pure diffusion and block/semi-AR sampling) under a unified training objective (Nie et al., 2025).

2.2 Latent-space reasoning and semantic-unit generation

A growing line of work argues that allocating computation in *latent* representations can improve reasoning by delaying irreversible surface-form decisions (Hao et al., 2024). Continuous latent reasoning approaches train models to perform intermediate computation in a learned continuous space and decode to text only at the end (Zhu et al., 2025). Related directions study how latent structures can be induced or discovered to support reasoning behavior, such as latent skill discovery for chain-of-thought reasoning (Xu et al., 2023).

Complementary to latent reasoning, recent work explores operating over higher-level semantic units (“concepts”) rather than tokens. A parallel work, Dynamic Large Concept Models explicitly model and generate sequences of large semantic con-

cepts to reduce token-level burden and improve efficiency (Qu et al., 2025). VDLM follows this spirit but focuses on *diffusion-time semantic revision*: masked diffusion is applied to a fixed-length sequence of variable slots in continuous space, and long text is recovered by a separate renderer.

2.3 Reinforcement learning for diffusion language models

Post-training diffusion LMs with reinforcement learning is non-trivial because generation is a multi-step denoising trajectory; effective credit assignment should respect the *inference trace*. TRACERL addresses this by introducing trajectory-aware objectives and diffusion-aware value modeling to stabilize RL for diffusion generation (Wang et al., 2025b). (Wang et al., 2025a) proposes a principled RL framework for masked DLMs, deriving policy-gradient estimators that explicitly rely on sampling-trajectory likelihood computation

We adapt TraceRL-style ideas to *variable diffusion* and further reduce training cost by computing rewards and values directly in embedding space, avoiding text rendering inside the RL loop.

2.4 Embedding inversion and Vec2Text rendering

Embedding inversion studies how much information is preserved in text embedding models and how to recover text from dense vectors. VEC2TEXT shows that modern embeddings retain substantial recoverable signal and proposes a hypothesizer-corrector architecture that iteratively refines a decoded hypothesis by comparing its embedding to the target (Morris et al., 2023a). Vec2Text is commonly trained to invert strong embedders such as GTR-style encoders (Morris et al., 2023a,b). In practice, however, inversion can be brittle under off-manifold or noisy embeddings. Recent results further suggest that transformer representations can be injective and exactly invertible, enabling provable input reconstruction from hidden activations (Nikolaou et al., 2025). CALM thus improves robustness of language autoencoders by training the encoder-decoder with variational regularization and noise injection so that decoding remains stable under perturbations in the continuous latent space (Shao et al., 2025).

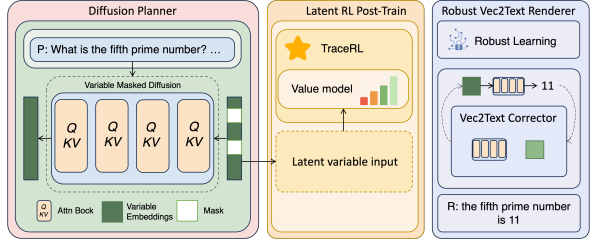


Figure 1: **VDLM pipeline overview.** A variable-level diffusion planner refines semantic variable embeddings via masked denoising; the planner is post-trained with TraceRL-style trajectory-aware RL entirely in latent space (reward/value computed from embeddings, no text decoding in the RL loop); an robustly trained Vec2Text renderer robustly converts the final latent plan into text under planner-induced embedding noise.

3 Method

3.1 Overview

Given an input p , we construct a fixed-length sequence of semantic variables $\tilde{V} = [\tilde{v}_1, \dots, \tilde{v}_n]$ (e.g., prompt parts, options, or steps), pad to N_{\max} , and embed each variable into a continuous vector. We train a shared conditional denoiser to recover masked variables in embedding space (**Stage I**) and then finetune it with TraceRL-style reward RL for downstream tasks (**Stage II**) from the Stage I checkpoint. Finally, a VEC2TEXT renderer decodes the planned embeddings to text (**Stage III**); it is trained separately using paired text-embedding data from a frozen encoder $E(\cdot)$, with noise injected to ensure robustness. No gradients are propagated from the renderer back into the planner/encoder unless stated otherwise.

3.2 Variable construction and embedding

We obtain semantic variables by a lightweight segmentation function $\text{Split}(\cdot)$ that produces $n \leq N_{\max}$ text spans:

$$\begin{aligned} \tilde{V} &= \text{Split}(p) = [\tilde{v}_1, \dots, \tilde{v}_n] \\ n &= |\tilde{V}| \leq N_{\max}, \end{aligned} \tag{1}$$

where each \tilde{v}_i is a sequence of tokens.

Text-to-latent variable embedding. We embed each text span using a pretrained frozen encoder E (token encoder) and a trainable projection:

$$\begin{aligned} H_i &= E(\tilde{v}_i) \in \mathbb{R}^{\ell_i \times d_e}, \\ u_i &= \text{pool}(H_i) \in \mathbb{R}^{d_e}, \\ \bar{v}_i &= \text{Proj}(u_i) \in \mathbb{R}^d, \end{aligned} \tag{2}$$

Padding and stop mask. We pad into fixed slots $V = [v_1, \dots, v_{N_{\max}}] \in \mathbb{R}^{N_{\max} \times d}$ with a stop mask $s \in \{0, 1\}^{N_{\max}}$:

$$v_i = \begin{cases} \bar{v}_i, & i \leq n, \\ \mathbf{0} \in \mathbb{R}^d, & i > n, \end{cases} \quad s_i = \begin{cases} 1, & i \leq n, \\ 0, & i > n. \end{cases} \quad (3)$$

3.3 Conditional masked denoiser (LLaDA-style)

Let $V^0 \in \mathbb{R}^{N_{\max} \times d}$ be the clean variable embeddings. We learn a mask embedding $m \in \mathbb{R}^d$ and mask a subset of *active* slots $\mathcal{M} \subseteq \{i : s_i = 1\}$:

$$V_i^t = \begin{cases} m & i \in \mathcal{M}, \\ V_i^0 & \text{otherwise.} \end{cases} \quad (4)$$

We also encode the full problem prompt into token states $P \in \mathbb{R}^{m \times d}$ and apply cross-attention at each layer. The denoiser Θ predicts clean embeddings and stop probabilities:

$$(\hat{V}^0, \hat{s}) = \Theta(V^t, P), \quad (5)$$

where $\hat{V}^0 \in \mathbb{R}^{N_{\max} \times d}$ and $\hat{s} \in [0, 1]^{N_{\max}}$.

3.4 Stage I: LLaDA style reconstruction pretraining

We sample a masking rate $t \sim \text{Uniform}(0, 1)$ and mask each active slot with probability t . Reconstruction is applied only to masked active positions:

$$\mathcal{L}_{\text{recon}} = \mathbb{E} \left[\sum_{i=1}^{N_{\max}} \mathbf{1}[i \in \mathcal{M}] \cdot \|\hat{V}_i^0 - V_i^0\|_2^2 \right]. \quad (6)$$

Stop-mask supervision uses BCE:

$$\begin{aligned} \mathcal{L}_{\text{stop}} &= \mathbb{E} \left[\sum_{i=1}^{N_{\max}} \text{BCE}(\hat{s}_i, s_i) \right], \\ \mathcal{L}_{\text{pre}} &= \mathcal{L}_{\text{recon}} + \lambda_{\text{stop}} \mathcal{L}_{\text{stop}}. \end{aligned} \quad (7)$$

More details can refer to (Nie et al., 2025)

3.5 Stage II: TraceRL-style RL in latent (embedding) space

We finetune the denoiser parameters Θ_p to directly optimize task reward using a **trajectory-aware policy optimization** objective (Wang et al., 2025b). In this work, both the *reward head* and the *value model* operate on latent variable embeddings rather than the tokens. Therefore the RL loop does *not* require text decoding or rendering.

Latent diffusion trajectory. Conditioned on an input p , the reverse process induces a latent trajectory $\tau = (V_T, V_{T-1}, \dots, V_0)$ in continuous space. At each reverse step $t \in \{T, \dots, 1\}$, we sample the next latent state from a Gaussian centered at the denoiser prediction:

$$\begin{aligned} V_{t-1} &\sim \pi_{\Theta_p}(\cdot | V_t, p, t) = \mathcal{N}(\mu_{\Theta_p}(V_t, p, t), \Sigma_t) \\ \log \pi_{\Theta_p}(V_{t-1} | V_t, p, t) &= -\frac{1}{2} \|V_{t-1} - \mu_{\Theta_p}(V_t, p, t)\|_{\Sigma_t^{-1}}^2 \\ &\quad + \text{const}, \end{aligned} \quad (8)$$

where μ_{Θ_p} is parameterized by the denoiser and Σ_t follows the diffusion schedule.

Reward head in embedding space. We compute a scalar reward $r \in [0, 1]$ from the *final* latent output V_0 using a lightweight scoring rule. For multiple-choice tasks, we score each candidate option by cosine similarity to a predicted *answer embedding* and take an argmax. For exact-match style tasks, we threshold similarity between a predicted *final embedding* and the gold answer embedding. In the verifiable-reward setting, we use terminal-only reward: $r_0 = r$ and $r_t = 0$ for $t > 0$.

Trajectory-aware PPO objective We follow TraceRL’s **trajectory-aware PPO** objective with trace shrink. Let π_{old} be a frozen snapshot used to collect rollouts, and define the transition density ratio for each step:

$$\rho_t(\Theta_p) = \frac{\pi_{\Theta_p}(V_{t-1} | V_t, p, t)}{\pi_{\text{old}}(V_{t-1} | V_t, p, t)}. \quad (9)$$

We maximize the clipped surrogate with a KL penalty (Schulman et al., 2017):

$$\begin{aligned} J_{\text{policy}}(\Theta_p) &= \mathbb{E}_p \mathbb{E}_{\tau \sim \pi_{\text{old}}(\cdot | p)} \left[\frac{\sum_{t \in \tau^{(s)}} C_{\epsilon}(\rho_t(\Theta_p), A_t)}{|\tau^{(s)}|} \right. \\ &\quad \left. - \beta \text{KL}(\pi_{\Theta_p} \| \pi_{\text{old}}) \right], \\ C_{\epsilon}(\rho, A) &= \min \left(\rho A, \text{clip}(\rho, 1 - \epsilon, 1 + \epsilon) A \right). \end{aligned} \quad (10)$$

and minimize $\mathcal{L}_{\text{RL}} = -J_{\text{policy}}(\Theta_p)$ as the loss function. When using terminal-only verifiable rewards, we set $A_t \equiv A$ (shared across the trajectory) by default, matching TraceRL’s efficient RLVR regime (Wang et al., 2025b).

Latent-space value model and advantages. We train a value network V_{Θ_v} in latent space to reduce variance and match the output of the diffusion model. The value model takes (V_t, p, t) and

predicts a step-wise value estimate $V_{\Theta_v, t}$. We compute advantages with GAE/TD(λ) (Schulman et al., 2015) over reverse steps:

$$\delta_t = r_t + \gamma V_{\text{old}, t-1} - V_{\text{old}, t}, \quad (11)$$

$$A_t = \delta_t + \gamma \lambda A_{t-1}, \quad (12)$$

with terminal conditions consistent with reverse-time indexing.

Clipped value regression. We train V_{Θ_v} with a clipped regression objective following TraceRL:

$$\begin{aligned} J_{\text{value}}(\Theta_v) = \frac{1}{2} \mathbb{E}_p \mathbb{E}_{\tau \sim \pi_{\text{old}}(\cdot | p)} \left[\frac{1}{|\tau^{(s)}|} \sum_{t \in \tau^{(s)}} \right. \\ \max \left((V_{\Theta_v, t} - R_t)^2, \right. \\ \left. \left. (V_t^{\text{clip}} - R_t)^2 \right) \right], \\ V_t^{\text{clip}} = V_{\text{old}, t} + \text{clip}(V_{\Theta_v, t} - V_{\text{old}, t}, -\epsilon, \epsilon). \end{aligned} \quad (13)$$

where R_t is the return defined by the chosen reward assignment. More details can be found in (0)

Overall optimization. We alternate between (i) updating Θ_p via (10) and (ii) updating Θ_v via (13). We standardize advantages within a minibatch and tune $(\epsilon, \beta, \gamma, \lambda)$ for stability, following TraceRL (Wang et al., 2025b).

3.6 Stage III: Rendering with Robust Vec2Text

We render the final planned variable embeddings into text using VEC2TEXT (Morris et al., 2023a), an embedding-inversion model based on an iterative hypothesizer-corrector paradigm. The inverse map from a dense embedding to a discrete token sequence is inherently brittle: small perturbations in embedding space can induce discontinuous changes in the decoded text, and planner outputs may drift off the embedder’s manifold. Unlike image diffusion, where a continuous decoder maps latents to pixels, text rendering must reconstruct a discrete sequence and is therefore especially sensitive to noise.

Robust Training To bridge the distribution gap between training-time embeddings and noisy planner outputs, we robustify the Vec2Text corrector through noise injection. Given a planned variable embedding v , we inject L_2 noise

$$v' = v + \epsilon, \quad \epsilon \sim \mathcal{N}(0, \alpha^2 I), \quad (14)$$

and train the corrector to recover the exact target answer text from v' (details in Appendix D). Concretely, we minimize the standard sequence negative log-likelihood conditioned on the perturbed embedding:

$$\mathcal{L}_{\text{render}} = -\mathbb{E}_{(x, v)} \mathbb{E}_{\epsilon \sim \mathcal{N}(0, \alpha^2 I)} \left[\log p_{\psi}(x | v', \text{ctx}) \right], \quad (15)$$

where ctx denotes the corrector’s auxiliary conditioning (e.g., the current hypothesis and its embedding). This robust training substantially improves robustness for long variable segments and is a key driver of our rendering gains over semi-autoregressive alternatives.

4 Experiments

4.1 Setup

Benchmarks. We evaluate on nine standard benchmarks spanning general knowledge/reasoning, math/science, and code: MMLU (Hendrycks et al., 2021a), BBH (Suzgun et al., 2022), ARC-Challenge (Clark et al., 2018), TruthfulQA (Lin et al., 2022), PIQA (Bisk et al., 2019) (general); GSM8K (Cobbe et al., 2021), MATH (Hendrycks et al., 2021b), GPQA (Rein et al., 2023) (math/science); and HumanEval (Chen et al., 2021) (code). We follow LLaDA (Nie et al., 2025) for few-shot prompting.

Baseline. Our primary diffusion language model baseline is LLaDA 8B (Nie et al., 2025) under (i) pure diffusion decoding and (ii) the semi-autoregressive / block diffusion sampling variant provided in the same work. We also contextualize results against strong AR models (LLaMA3 8B (Chen et al., 2021), Qwen2/2.5 7B (Yang et al., 2024; Qwen et al., 2025), Mistral 7B (Jiang et al., 2023), DeepSeek 7B (Jiang et al., 2023), Gemma2 9B (Team et al., 2024)) using the numbers reported in prior work. As in LLaDA-style reporting, we distinguish *same-protocol* evaluations (*) from sourced results to avoid overstating strict comparability.

VDLM implementation (planner + renderer). VDLM consists of (i) a *variable diffusion planner* (22-layer Transformer denoiser, $d=2048$) and (ii) an *Robust-Vec2Text renderer* built on the Vec2Text inversion framework (Morris et al., 2023a) with a default LLaMA 3 8B (instruct) embedding encoder. Training proceeds in three stages: **Stage I**

masked diffusion pretraining ; **Stage II** TraceRL-style RL in embedding space (no decoding inside the RL loop) (Wang et al., 2025b); **Stage III** renderer training with noise perturbations. Unless stated otherwise, we run Vec2Text correction for $L' = 10$ iterations at inference.

4.2 Main Results

Pre-training. Table 1 reports pre-trained results across nine benchmarks. Among the models evaluated under the same protocol (*), VDLM achieves the highest average score (51.6), outperforming LLaDA by 2.3 points (49.3). VDLM improves over LLaDA on MMLU (+5.5), BBH (+4.8), ARC-C (+8.5), and TruthfulQA (+4.1), while matching PIQA. These gains show that diffusion-time refinement in a semantic latent space can preserve the capabilities of token-space diffusion while reducing training and memory costs.

On mathematical reasoning, VDLM reaches 66.6 on GSM8K and 35.3 on MATH. Relative to LLaDA, VDLM is slightly lower on GSM8K (-3.7) but higher on MATH (+3.9). On HumanEval, VDLM trails LLaDA (31.9 vs. 35.4), suggesting code generation remains a challenging regime for the current renderer, motivating code-specialized rendering or post-training.

Post-training. Table 2 reports post-trained results. VDLM employs SFT followed by TraceRL-style RL in embedding space (Wang et al., 2025b), while LLaDA uses SFT only. VDLM improves substantially on generation-heavy tasks: GSM8K increases from 66.6 to 89.8 (+23.2), MATH from 35.3 to 62.4 (+27.1), and HumanEval from 31.9 to 74.9 (+43.0). This confirms that the post-training recipe substantially improves downstream task performance in our setting, highlighting that embedding-space diffusion post-training is an effective approach.

VDLM narrows the gap with leading AR models. On GSM8K, VDLM (89.8) approaches Qwen2.5-7B and outperforms LLaMA3-8B Instruct (78.3) by +11.5 points. On MATH, VDLM (62.4) surpasses Qwen2-7B (52.9) by +9.5 points and Gemma2-9B (44.3) by +18.1 points, though it trails Qwen2.5-7B (75.5). Among diffusion models evaluated under the same protocol (*), VDLM outperforms LLaDA by +20.4 on GSM8K and +30.5 on MATH.

Code generation benefits from post-training. VDLM achieves 74.9 on HumanEval, a +43.0 point improvement over pre-trained VDLM (31.9). This

result demonstrates that embedding-space RL can effectively optimize for structured output generation, closing the gap with AR models.

4.3 Ablations and Analysis

We conduct ablations on three design choices that are central to VDLM’s performance: (1) the encoder backbone architecture, (2) the number of Vec2Text correction iterations, (3) the role of robust training, and (4) the influence of noise level.

Vec2Text iteration budget. Table 3 varies the number of Vec2Text correction iterations L' . Performance improves monotonically from $L' = 1$ to 20, with gains saturating around $L' = 20$.

The magnitude of improvement differs substantially by task type. For the short-output task MMLU, increasing iterations from $L' = 1$ to $L' = 10$ yields a +18.3 point gain. In contrast, long-output tasks exhibit much larger improvements: GSM8K gains +19.1 points, MATH gains +24.2 points, and HumanEval gains +27.5 points. Notably, the marginal returns diminish at higher iteration counts. $L' = 20$ approaches the reconstruction ceiling for the current Vec2Text model, and further gains would require improving the renderer itself rather than adding iterations.

This pattern supports the hypothesis that iterative correction primarily mitigates accumulated reconstruction error on long outputs. For multiple-choice tasks like MMLU, a single decoding pass captures most of the signal since outputs are short. However, for multi-step reasoning (GSM8K, MATH) and code generation (HumanEval), where outputs span dozens of tokens, the iterative refinement of Vec2Text becomes critical—each correction step reduces embedding-to-text drift that compounds over longer sequences.

Renderer robustness Table 4 isolates the impact of robust rendering. Vanilla Vec2Text (trained only on clean inversions) performs poorly when decoding planner-produced embeddings, while Robust-Vec2Text (trained with L_2 perturbations) substantially improves GSM8K/MATH/HumanEval. This supports the central claim that *robust latent-to-text rendering* is a key bottleneck for diffusion-style pipelines when the latent is imperfect at inference.

Embedding encoder backbone. Table 5 shows that VDLM benefits strongly from higher-quality embedding spaces. Using a weak encoder (T5-Base) yields poor results, while stronger encoders

Table 1: **Benchmark Results (Pre-training).** VDLM (variable diffusion + Vec2Text) on 9 benchmarks. * indicates that models are evaluated under the same protocol. The numbers in parentheses represent the number of shots used for in-context learning. “-” indicates unknown.

Benchmark	VDLM* Diffusion	LLaDA* Diffusion	LLaMA3 AR 8B	Qwen2 7B	Qwen2.5 7B	Mistral 7B	Deepseek 7B
<i>General Tasks</i>							
MMLU (5)	71.4	65.9	65.4	70.3	74.2	64.2	48.2
BBH (3)	54.5	49.7	62.1	62.3	70.4	56.1	39.5
ARC-C (0)	54.4	45.9	53.1	60.6	63.7	60.0	48.1
TruthfulQA (0)	50.2	46.1	44.0	54.2	56.4	42.2	57.4
PIQA (0)	74.2	73.6	80.6	—	—	—	79.2
<i>Mathematics & Science</i>							
GSM8K (4)	66.6	70.3	48.7	80.2	85.4	36.2	17.4
MATH (4)	35.3	31.4	16.0	43.5	49.8	10.2	6.0
GPQA (5)	25.6	25.2	25.9	30.8	36.4	24.7	—
<i>Code</i>							
HumanEval (0)	31.9	35.4	34.8	51.2	57.9	29.3	26.2

Table 2: **Benchmark Results (Post-training).** VDLM employs SFT and RL, while LLaDA uses SFT only; other models include RL alignment. * indicates models evaluated under the same protocol.

Model	Post-train	General Tasks			Math & Science		Code
		MMLU (5)	MMLU-Pro (0)	ARC-C (0)	GSM8K (4)	MATH (4)	HumanEval (0)
<i>Diffusion Models</i>							
VDLM*	SFT+RL	73.9	47.8	80.8	89.8	62.4	74.9
TraDo 8B*	SFT+RL	—	—	—	92.3	—	—
LLaDA 8B*	SFT	65.5	37.0	88.5	69.4	31.9	49.4
<i>Autoregressive Models</i>							
LLaMA3 8B*	SFT+RL	68.4	41.9	82.4	78.3	29.6	59.8
Qwen2 7B [†]	SFT+RL	—	44.1	—	85.7	52.9	79.9
Qwen2.5 7B [†]	SFT+RL	—	56.3	—	91.6	75.5	84.8
Gemma2 9B [†]	SFT+RL	—	52.1	—	76.7	44.3	68.9
Deepseek 7B [†]	SFT+RL	49.4	—	49.4	63.0	15.8	48.2

markedly improve downstream accuracy. We include OpenAI’s text-embedding-ada-002 as a widely used embedding baseline (Lin et al., 2023). Further gains emerge from open-weight LLM-based encoders. LLaMA3-8B embeddings achieve 89.8 / 62.4 / 74.9 on GSM8K / MATH / HumanEval, improving over ada-002 by +7.1 / +3.5 points on the math benchmarks while slightly trailing on HumanEval (-4.0). The strongest results come from the reasoning model’, Qwen3-Embedding-8B. These results show 1) VDLM can leverage future advances in embedding models. 2) the performance gap between T5-Base and Qwen3-Embedding underscores that the semantic structure of the latent space is not incidental but fundamental to enabling effective diffusion-time reasoning.

Noise Level Table 6 varies the noise level α used during robust training of Vec2Text. The result shows too little noise leaves the renderer brittle to planner outputs, while excessive noise degrades the learning signal. The optimal noise level is $\alpha = 0.01$. This configuration improves over the lowest noise setting ($\alpha = 0.001$) by +34.2 / +14.2 / +25.8 points respectively.

5 Discussion

Renderer as the dominant failure mode. Across our ablations, performance is far more sensitive to the rendering backbone than to the diffusion planner itself. Vanilla embedding inversion is brittle under planner-produced noise, and the gap closed by Robust-Vec2Text indicates that *ro-*

Table 3: **Ablation on number of iteration for Vec2Text.** L' is the number of iteration

		MMLU	GSM8K	Math	HumanEval
VDLM	$L' = 1$	55.6	70.7	38.2	47.4
	$L' = 3$	68.4	80.3	57.6	64.2
	$L' = 5$	72.6	86.5	62.1	70.3
	$L' = 10$	73.9	89.8	62.4	74.9
	$L' = 20$	74.1	89.8	62.5	75.3

Table 4: **Ablation on modules for VLDM**

	GSM8K	Math	HumanEval
Block Diffusion LLaDA	77.5	42.2	46.3
Vec2Text	46.2	32.3	44.2
Robust-Vec2Text	89.8	62.4	74.9

Table 5: **Ablation on Encoder Corrector Backbone**

	GSM8K	Math	HumanEval
T5-Base	32.0	12.3	15.7
text-embedding-ada-002	82.7	58.9	78.9
LLAMA3-8B-instruct	89.8	62.4	74.9
Qwen3-Embedding-8B	92.1	72.0	80.4

busness to embeddings is a first-order requirement for latent-variable diffusion LMs. This perspective also helps interpret why semi-AR/ block diffusion can degrade when segments grow: local decoding errors become harder to revise as the effective “block” of committed content increases, whereas iterative correction in embedding space explicitly revisits the entire hypothesis over multiple rounds.

RL aligns the tasks. Stage II optimizes rewards directly on variable embeddings, avoiding rendering inside the RL loop. This design trades token-level supervision for a faster optimization inner-loop, which is especially relevant when the renderer is large and iterative. At the same time, it introduces a new alignment question: the planner is optimized against an embedding-space scoring rule, so the renderer must faithfully map the optimized embeddings back to text. Our results suggest this coupling is workable when the renderer is robustified, but it remains an important axis for future controlled study.

Relation to emerging “latent reasoning” directions. Recent work has argued that decoupling internal reasoning states from token generation can improve efficiency and/or capability, by letting models do computation in a compact latent space before producing text. Our findings are con-

Table 6: **Ablation on noise level for Vec2Text.** α is the noise level

	GSM8K	Math	HumanEval
$\alpha = 0.001$	45.6	48.2	49.1
$\alpha = 0.005$	78.3	57.6	61.0
$\alpha = 0.01$	89.8	62.4	74.9
$\alpha = 0.02$	80.2	61.7	71.1
$\alpha = 0.05$	76.6	54.3	62.8

sistent with this thesis: when the latent space is semantically meaningful and the renderer is strong, latent-space refinement plus decoding can be competitive despite smaller trainable planning capacity. We view VDLM as complementary to these lines of work: rather than introducing an opaque latent, we use explicit variable slots and a separately trained renderer, enabling targeted robustness training and modular encoder upgrades.

Limitations. Math/code generation remains challenging in the pre-trained setting, indicating that embedding inversion may not preserve syntactic exactness as reliably as natural language. renderer specialization is a natural next step. Also, post-training improves GSM8K/MATH/HumanEval, further study in the post-training mechanism is required for the future work.

6 Conclusion

We introduced **VDLM**, a modular variable diffusion language model that separates semantic planning from text rendering. VDLM applies LLaDA-style masked diffusion over semantic variable embeddings, post-trains the planner with TraceRL-style trajectory optimization using *embedding-space* rewards/values, and renders via **Vec2Text** with **embedding perturbations** for robustness to planner noise. Across nine benchmarks, VDLM is competitive pre-training and achieves strong post-training gains on long-form generation; ablations show that robust rendering and embedding quality are key drivers.

References

Josh Achiam, Steven Adler, Sandhini Agarwal, Lama Ahmad, Ilge Akkaya, Florencia Leoni Aleman, Diogo Almeida, Janko Altenschmidt, Sam Altman, Shyamal Anadkat, and 1 others. 2023. Gpt-4 technical report. *arXiv preprint arXiv:2303.08774*.

Kushal Arora, Layla El Asri, Hareesh Bahuleyan, and Jackie Chi Kit Cheung. 2022. Why exposure bias matters: An imitation learning perspective of error accumulation in language generation. In *Findings of the Association for Computational Linguistics: ACL 2022*, pages 700–710.

Jacob Austin, Daniel D Johnson, Jonathan Ho, Daniel Tarlow, and Rianne Van Den Berg. 2021. Structured denoising diffusion models in discrete state-spaces. *Advances in neural information processing systems*, 34:17981–17993.

Tiwei Bie, Maosong Cao, Kun Chen, Lun Du, Mingliang Gong, Zhuochen Gong, Yanmei Gu, Jiaqi Hu, Zenan Huang, Zhenzhong Lan, and 1 others. 2025. Llada2. 0: Scaling up diffusion language models to 100b. *arXiv preprint arXiv:2512.15745*.

Yonatan Bisk, Rowan Zellers, Ronan Le Bras, Jianfeng Gao, and Yejin Choi. 2019. Piqa: Reasoning about physical commonsense in natural language. *Preprint*, arXiv:1911.11641.

Tom Brown, Benjamin Mann, Nick Ryder, Melanie Subbiah, Jared D Kaplan, Prafulla Dhariwal, Arvind Neelakantan, Pranav Shyam, Girish Sastry, Amanda Askell, and 1 others. 2020. Language models are few-shot learners. *Advances in neural information processing systems*, 33:1877–1901.

Mark Chen, Jerry Tworek, Heewoo Jun, Qiming Yuan, Henrique Ponde de Oliveira Pinto, Jared Kaplan, Harri Edwards, Yuri Burda, Nicholas Joseph, Greg Brockman, Alex Ray, Raul Puri, Gretchen Krueger, Michael Petrov, Heidy Khlaaf, Girish Sastry, Pamela Mishkin, Brooke Chan, Scott Gray, and 39 others. 2021. Evaluating large language models trained on code. *Preprint*, arXiv:2107.03374.

Shuang Cheng, Yihan Bian, Dawei Liu, Linfeng Zhang, Qian Yao, Zhongbo Tian, Wenhui Wang, Qipeng Guo, Kai Chen, Biqing Qi, and 1 others. 2025. Sdar: A synergistic diffusion-autoregression paradigm for scalable sequence generation. *arXiv preprint arXiv:2510.06303*.

Peter Clark, Isaac Cowhey, Oren Etzioni, Tushar Khot, Ashish Sabharwal, Carissa Schoenick, and Oyvind Tafjord. 2018. Think you have solved question answering? try arc, the AI2 reasoning challenge. *CoRR*, abs/1803.05457.

Karl Cobbe, Vineet Kosaraju, Mohammad Bavarian, Mark Chen, Heewoo Jun, Lukasz Kaiser, Matthias Plappert, Jerry Tworek, Jacob Hilton, Reiichiro Nakano, Christopher Hesse, and John Schulman. 2021. Training verifiers to solve math word problems. *Preprint*, arXiv:2110.14168.

Shibo Hao, Sainbayar Sukhbaatar, DiJia Su, Xian Li, Zhiting Hu, Jason Weston, and Yuandong Tian. 2024. Training large language models to reason in a continuous latent space. *arXiv preprint arXiv:2412.06769*.

Tianxing He, Jingzhao Zhang, Zhiming Zhou, and James Glass. 2021. Exposure bias versus self-recovery: Are distortions really incremental for autoregressive text generation? In *Proceedings of the 2021 Conference on Empirical Methods in Natural Language Processing*, pages 5087–5102.

Zhengfu He, Tianxiang Sun, Qiong Tang, Kuanning Wang, Xuan-Jing Huang, and Xipeng Qiu. 2023. Diffusionbert: Improving generative masked language models with diffusion models. In *Proceedings of the 61st annual meeting of the association for computational linguistics (volume 1: Long papers)*, pages 4521–4534.

Dan Hendrycks, Collin Burns, Steven Basart, Andy Zou, Mantas Mazeika, Dawn Song, and Jacob Steinhardt. 2021a. Measuring massive multitask language understanding. *Proceedings of the International Conference on Learning Representations (ICLR)*.

Dan Hendrycks, Collin Burns, Saurav Kadavath, Akul Arora, Steven Basart, Eric Tang, Dawn Song, and Jacob Steinhardt. 2021b. Measuring mathematical problem solving with the math dataset. *Preprint*, arXiv:2103.03874.

Jonathan Ho, Ajay Jain, and Pieter Abbeel. 2020. Denoising diffusion probabilistic models. *Advances in neural information processing systems*, 33:6840–6851.

Jie Huang, Xinyun Chen, Swaroop Mishra, Huaixiu Steven Zheng, Adams Wei Yu, Xinying Song, and Denny Zhou. 2023. Large language models cannot self-correct reasoning yet, 2024. *arXiv preprint arXiv:2310.01798*.

Daniel Israel, Guy Van den Broeck, and Aditya Grover. Accelerating diffusion llms via adaptive parallel decoding, 2025. URL <https://arxiv.org/abs/2506.00413>, 3.

Albert Q. Jiang, Alexandre Sablayrolles, Arthur Mensch, Chris Bamford, Devendra Singh Chaplot, Diego de las Casas, Florian Bressand, Gianna Lengyel, Guillaume Lample, Lucile Saulnier, Lélio Renard Lavaud, Marie-Anne Lachaux, Pierre Stock, Teven Le Scao, Thibaut Lavril, Thomas Wang, Timothée Lacroix, and William El Sayed. 2023. **Mistral 7b**. *Preprint*, arXiv:2310.06825.

Xiang Li, John Thickstun, Ishaan Gulrajani, Percy S Liang, and Tatsunori B Hashimoto. 2022. Diffusion-lm improves controllable text generation. *Advances in neural information processing systems*, 35:4328–4343.

Jimmy Lin, Ronak Pradeep, Tommaso Teofili, and Jasper Xian. 2023. Vector search with openai embeddings: Lucene is all you need. *Preprint*, arXiv:2308.14963.

Stephanie Lin, Jacob Hilton, and Owain Evans. 2022. [Truthfulqa: Measuring how models mimic human falsehoods](#). *Preprint*, arXiv:2109.07958.

Guanxi Lu, Hao Mark Chen, Yuto Karashima, Zhi-can Wang, Daichi Fujiki, and Hongxiang Fan. 2025. Adablock-dllm: Semantic-aware diffusion llm inference via adaptive block size. *arXiv preprint arXiv:2509.26432*.

Shervin Minaee, Tomas Mikolov, Narjes Nikzad, Meysam Chenaghlu, Richard Socher, Xavier Amatriain, and Jianfeng Gao. 2024. Large language models: A survey. *arXiv preprint arXiv:2402.06196*.

John Morris, Volodymyr Kuleshov, Vitaly Shmatikov, and Alexander M Rush. 2023a. Text embeddings reveal (almost) as much as text. In *Proceedings of the 2023 Conference on Empirical Methods in Natural Language Processing*, pages 12448–12460.

John X. Morris, Wenting Zhao, Justin T. Chiu, Vitaly Shmatikov, and Alexander M. Rush. 2023b. [Language model inversion](#). *Preprint*, arXiv:2311.13647.

Shen Nie, Fengqi Zhu, Zebin You, Xiaolu Zhang, Jingyang Ou, Jun Hu, Jun Zhou, Yankai Lin, Ji-Rong Wen, and Chongxuan Li. 2025. Large language diffusion models. *arXiv preprint arXiv:2502.09992*.

Giorgos Nikolaou, Tommaso Mencattini, Donato Crisostomi, Andrea Santilli, Yannis Panagakis, and Emanuele Rodolà. 2025. Language models are injective and hence invertible. *arXiv preprint arXiv:2510.15511*.

William Peebles and Saining Xie. 2023. Scalable diffusion models with transformers. In *Proceedings of the IEEE/CVF international conference on computer vision*, pages 4195–4205.

Mihir Prabhudesai, Mengning Wu, Amir Zadeh, Katerina Fragkiadaki, and Deepak Pathak. 2025. Diffusion beats autoregressive in data-constrained settings. *arXiv preprint arXiv:2507.15857*.

Xingwei Qu, Shaowen Wang, Zihao Huang, Kai Hua, Fan Yin, Rui-Jie Zhu, Jundong Zhou, Qiyang Min, Zihao Wang, Yizhi Li, and 1 others. 2025. Dynamic large concept models: Latent reasoning in an adaptive semantic space. *arXiv preprint arXiv:2512.24617*.

Qwen, :, An Yang, Baosong Yang, Beichen Zhang, Binyuan Hui, Bo Zheng, Bowen Yu, Chengyuan Li, Dayiheng Liu, Fei Huang, Haoran Wei, Huan Lin, Jian Yang, Jianhong Tu, Jianwei Zhang, Jianxin Yang, Jiaxi Yang, Jingren Zhou, and 25 others. 2025. [Qwen2.5 technical report](#). *Preprint*, arXiv:2412.15115.

Colin Raffel, Noam Shazeer, Adam Roberts, Katherine Lee, Sharan Narang, Michael Matena, Yanqi Zhou, Wei Li, and Peter J. Liu. 2023. [Exploring the limits of transfer learning with a unified text-to-text transformer](#). *Preprint*, arXiv:1910.10683.

David Rein, Betty Li Hou, Asa Cooper Stickland, Jackson Petty, Richard Yuanzhe Pang, Julien Diranji, Julian Michael, and Samuel R Bowman. 2023. GPQA: A graduate-level google-proof q&a benchmark. *arXiv preprint arXiv:2311.12022*.

Subham Sahoo, Marianne Arriola, Yair Schiff, Aaron Gokaslan, Edgar Marroquin, Justin Chiu, Alexander Rush, and Volodymyr Kuleshov. 2024. Simple and effective masked diffusion language models. *Advances in Neural Information Processing Systems*, 37:130136–130184.

Florian Schmidt. 2019. Generalization in generation: A closer look at exposure bias. *arXiv preprint arXiv:1910.00292*.

John Schulman, Philipp Moritz, Sergey Levine, Michael Jordan, and Pieter Abbeel. 2015. High-dimensional continuous control using generalized advantage estimation. *arXiv preprint arXiv:1506.02438*.

John Schulman, Filip Wolski, Prafulla Dhariwal, Alec Radford, and Oleg Klimov. 2017. Proximal policy optimization algorithms. *arXiv preprint arXiv:1707.06347*.

Chenze Shao, Darren Li, Fandong Meng, and Jie Zhou. 2025. Continuous autoregressive language models. *arXiv preprint arXiv:2510.27688*.

Mirac Suzgun, Nathan Scales, Nathanael Schärlí, Sebastian Gehrmann, Yi Tay, Hyung Won Chung, Aakanksha Chowdhery, Quoc V. Le, Ed H. Chi, Denny Zhou, and Jason Wei. 2022. [Challenging big-bench tasks and whether chain-of-thought can solve them](#). *Preprint*, arXiv:2210.09261.

Gemma Team, Morgane Riviere, Shreya Pathak, Pier Giuseppe Sessa, Cassidy Hardin, Surya Bhupatiraju, Léonard Hussenot, Thomas Mesnard, Bobak Shahriari, Alexandre Ramé, Johan Ferret, Peter Liu, Pouya Tafti, Abe Friesen, Michelle Casbon, Sabela Ramos, Ravin Kumar, Charline Le Lan, Sammy Jerome, and 179 others. 2024. [Gemma 2: Improving open language models at a practical size](#). *Preprint*, arXiv:2408.00118.

Hugo Touvron, Thibaut Lavril, Gautier Izacard, Xavier Martinet, Marie-Anne Lachaux, Timothée Lacroix, Baptiste Rozière, Naman Goyal, Eric Hambro, Faisal Azhar, and 1 others. 2023. Llama: Open and efficient foundation language models. *arXiv preprint arXiv:2302.13971*.

Chunqi Wang, Ji Zhang, and Haiqing Chen. 2018. Semi-autoregressive neural machine translation. *arXiv preprint arXiv:1808.08583*.

Guanghan Wang, Yair Schiff, Gilad Turok, and Volodymyr Kuleshov. 2025a. d2: Improved techniques for training reasoning diffusion language models. *arXiv preprint arXiv:2509.21474*.

Xuezhi Wang, Jason Wei, Dale Schuurmans, Quoc Le, Ed Chi, Sharan Narang, Aakanksha Chowdhery, and Denny Zhou. 2022. Self-consistency improves chain of thought reasoning in language models. *arXiv preprint arXiv:2203.11171*.

Yinjie Wang, Ling Yang, Bowen Li, Ye Tian, Ke Shen, and Mengdi Wang. 2025b. Revolutionizing reinforcement learning framework for diffusion large language models. *arXiv preprint arXiv:2509.06949*.

Jason Wei, Xuezhi Wang, Dale Schuurmans, Maarten Bosma, Fei Xia, Ed Chi, Quoc V Le, Denny Zhou, and 1 others. 2022. Chain-of-thought prompting elicits its reasoning in large language models. *Advances in neural information processing systems*, 35:24824–24837.

Zhen Xiong, Yujun Cai, Zhecheng Li, and Yiwei Wang. 2025. Unveiling the potential of diffusion large language model in controllable generation. *arXiv preprint arXiv:2507.04504*.

Zifan Xu, Haozhu Wang, Dmitriy Bespalov, Xuan Wang, Peter Stone, and Yanjun Qi. 2023. Latent skill discovery for chain-of-thought reasoning. *arXiv preprint arXiv:2312.04684*.

An Yang, Baosong Yang, Binyuan Hui, Bo Zheng, Bowen Yu, Chang Zhou, Chengpeng Li, Chengyuan Li, Dayiheng Liu, Fei Huang, Guanting Dong, Haoran Wei, Huan Lin, Jialong Tang, Jialin Wang, Jian Yang, Jianhong Tu, Jianwei Zhang, Jianxin Ma, and 43 others. 2024. *Qwen2 technical report. Preprint*, arXiv:2407.10671.

Shunyu Yao, Dian Yu, Jeffrey Zhao, Izhak Shafran, Tom Griffiths, Yuan Cao, and Karthik Narasimhan. 2023. Tree of thoughts: Deliberate problem solving with large language models. *Advances in neural information processing systems*, 36:11809–11822.

Jiacheng Ye, Zihui Xie, Lin Zheng, Jiahui Gao, Zirui Wu, Xin Jiang, Zhenguo Li, and Lingpeng Kong. 2025. Dream 7b: Diffusion large language models. *arXiv preprint arXiv:2508.15487*.

Runpeng Yu, Qi Li, and Xinchao Wang. 2025. Discrete diffusion in large language and multimodal models: A survey. *arXiv preprint arXiv:2506.13759*.

Hanlin Zhu, Shibo Hao, Zhiting Hu, Jiantao Jiao, Stuart Russell, and Yuandong Tian. 2025. Emergence of superposition: Unveiling the training dynamics of chain of continuous thought. *arXiv preprint arXiv:2509.23365*.

A Appendix Overview

We include implementation details, full preprocessing, extended ablations, and additional robustness experiments. This appendix is non-essential for the main narrative.

B Variable segmentation details

We use a simple segmentation function `Split` that produces variable chunks from the input text. Concretely, we split by whitespace-delimited line breaks and tab markers, steps, choice and etc, then enforce length bounds and pad to N_{\max} .

C Reward computation in embedding space

We compute reward without decoding to text during RL finetuning.

Multiple-choice. We embed candidate options with the same frozen encoder and select the argmax cosine similarity.

Exact match. We embed the gold answer string and compare against the predicted final embedding via cosine thresholding. We normalize thresholds on a held-out dev subset.

D Vec2Text Rendering Pipeline

This appendix summarizes the VEC2TEXT embedding-to-text inversion pipeline (Morris et al., 2023a) and specifies the losses used for the hypothesizer–corrector training.

D.1 Controlled generation view of embedding inversion

Let $\phi : \mathcal{X} \rightarrow \mathbb{R}^d$ be a frozen text embedder and let $e \in \mathbb{R}^d$ denote a target embedding. Vec2Text frames inversion as controlled generation, seeking text whose embedding matches e :

$$\hat{x} = \arg \max_x \cos(\phi(x), e). \quad (16)$$

D.2 Hypothesizer–corrector recursion

A one-shot inversion model $p(x | e)$ is often insufficient, so Vec2Text generates an initial hypothesis and iteratively refines it. Let $x^{(t)}$ be the hypothesis at iteration t and $\hat{e}^{(t)} = \phi(x^{(t)})$ its embedding. The correction process can be written as:

$$p(x^{(t+1)} | e) = \sum_{x^{(t)}} p(x^{(t)} | e) p(x^{(t+1)} | e, x^{(t)}, \hat{e}^{(t)}), \quad (17)$$

$$\hat{e}^{(t)} = \phi(x^{(t)}), \quad (18)$$

with base distribution (the hypothesizer)

$$p(x^{(0)} | e) = p(x^{(0)} | e, \emptyset, \phi(\emptyset)). \quad (19)$$

D.3 Training objectives

Base inversion (hypothesizer). Vec2Text trains an initial inversion model by maximum likelihood on paired text/embedding data:

$$\mathcal{L}_{\text{base}} = -\mathbb{E}_{x \sim \mathcal{D}} [\log p(x \mid \phi(x))]. \quad (20)$$

Corrector training. Given hypotheses $x^{(t)}$ (seeded from the base model), the corrector is trained with standard sequence NLL:

$$\mathcal{L}_{\text{corr}} = -\mathbb{E}_{x \sim \mathcal{D}} \mathbb{E}_{x^{(t)} \sim p(\cdot \mid \phi(x))} \left[\log p(x \mid \phi(x), x^{(t)}, \phi(x^{(t)})) \right]. \quad (21)$$

Robust training To handle noisy planner embeddings, we perturb the conditioning embedding and train the corrector to recover the ground-truth text:

$$v' = v + \epsilon, \quad \epsilon \sim \mathcal{N}(0, \alpha^2 I), \quad (22)$$

$$\mathcal{L}_{\text{render}} = -\mathbb{E}_{(x, v)} \mathbb{E}_{\epsilon \sim \mathcal{N}(0, \alpha^2 I)} \left[\log p_{\psi}(x \mid v', x^{(t)}, \phi(x^{(t)})) \right]. \quad (23)$$

In practice we apply this perturbation primarily to the corrector (not the base hypothesizer), since iterative correction is where robustness to embedding drift matters most for long variable segments.

E Implementation Details

E.1 Encoder configuration.

We use **LLaMA-3 8B Instruct** as the default encoder.

- **Model:** LLaMA-3 8B Instruct
- **Parameters:** 8B
- **Context length:** 8192 tokens
- **Hidden dimension:** 4096
- **Attention heads:** 32
- **Layers:** 32
- **Vocabulary:** 128,256 tokens

E.2 Vec2Text Module

For converting between embeddings and natural language (used in hypothesis generation and verification), we adopt a T5-based default decoder architecture (Raffel et al., 2023).

E.3 Vec2Text configuration.

- **Architecture:** T5 encoder-decoder
- **Model size:** T5-large
- **Decoder layers:** 22
- **Hidden dimension:** 2048
- **Feed-forward dimension:** 4096
- **Attention heads:** 16

E.4 DLM configuration.

- **Layers:** 22
- **Model dimension:** 2048
- **Attention heads:** 32
- **Feed-forward dimension:** 4096
- **Key/value heads:** 4 (grouped-query attention)

F AI Assistant Usage

This research utilized AI assistants including Claude and GPT-5 for several aspects of the paper and dataset preparation. We employed these tools mainly for:

- **Implementation support:** AI assistants provided code debugging assistance for the implementation and modification of dLLM, vec2text repos.
- **Manuscript preparation:** We used AI assistants for literature review to identify relevant papers, proofreading, language refinement, and formatting assistance.
- **Benchmark:** We use AI assistant GPT-5 to source some results from (Nie et al., 2025; Wang et al., 2025b).